

Preparation and reactivity of mono- and binuclear nitrosyl molybdenum complexes containing S_2CPCy_3 ligands. Crystal structure of $[(OC)_2(ON)Mo(\mu-Br)(\mu-S_2CPCy_3)Mo(CO)_2(PEt_3)]$

Daniel Miguel ^{a,*}, Víctor Riera ^a, Mei Wang ^a, Claudette Bois ^b, Yves Jeannin ^b

^a Instituto Universitario de Química Organometálica 'Enrique Moles', Unidad Asociada del CSIC, Universidad de Oviedo, E-33071 Oviedo, Spain

^b Laboratoire de Chimie des Métaux de Transition. UA-CNRS 419, Université Pierre et Marie Curie, 4 Place Jussieu, 75252 Paris Cedex 05, France

Received 17 March 1997

Abstract

A mononuclear nitrosyl complex with the S_2CPCy_3 ligand, $[MoBr(NO)(CO)_2(S_2CPCy_3)]$ (**3**), has been prepared from $[Mo(CO)_3(NCMe)_3]$ in three steps: (i) nitrosylation with an excess of $NOBF_4$, (ii) addition of bromide with Ph_4PBr or Et_4NBr , and (iii) ligand substitution by S_2CPCy_3 . Complex **3** readily reacts with $[M(CO)_3(NCR)_3]$ ($M = Mo, R = Me; M = W, R = Et$) to give binuclear nitrosyl complexes $[(OC)_2(ON)Mo(\mu-Br)(\mu-S_2CPCy_3)M(CO)_3]$ (**4a**, $M = Mo$; **4b**, $M = W$) containing $\eta^2(S,S')$; $\eta^3(S,C,S')$ - S_2CPR_3 , and bromide bridges. One carbonyl ligand from the ' $Mo(CO)_3$ ' fragment of the binuclear pentacarbonyl complex **4a** can be easily substituted by phosphine or phosphite ligands to give complexes $[(OC)_2(ON)Mo(\mu-Br)(\mu-S_2CPCy_3)Mo(CO)_2(L)]$ (**5a**: $L = PEt_3$; **5b**: $L = P(OMe)_3$). The single crystal X-ray diffraction study of **5a** shows that the central carbon atom of the S_2CPCy_3 ligand is bonded to the molybdenum atom of the ' $Mo(CO)_2(PEt_3)$ ' fragment, which is expected to be electron-richer. With potentially bidentate phosphine ligands ($L-L$), one CO ligand on the ' $Mo(CO)_3$ ' fragment of the binuclear complex **4a** was replaced and one of the $Mo(II)-S$ bonds was cleaved to afford complexes $[(OC)_2(ON)Mo(\mu-Br)(\mu-S_2CPCy_3)(\mu-L-L)Mo(CO)_2]$ (**6a**: $L-L = Me_2PCH_2PMe_2$; **6b**: $L-L = Ph_2PCH_2Ph_2$). © 1997 Elsevier Science S.A.

Keywords: Molybdenum; Tungsten; Nitrosyl complexes; Homo- and heterobimetallics; Trialkylphosphoniodithiocarboxylate ligands

1. Introduction

Although since the early 1980s the number of transition metal complexes containing S_2CPR_3 ligands has grown rapidly [1–10] and their chemical reactivities have been studied [11–16], nitrosyl transition metal complexes containing S_2CPR_3 ligands are limited to the mononuclear species reported by Carmona et al. [17]. To our knowledge, until now the effect of NO coordination on the chemical reactivities of the complexes containing S_2CPR_3 ligands remains unexplored. In many cases, it has been proved that the coordination of the nitrosyl ligand can result in change of the stability and

the chemical reactivity of the organometallic complexes, and that some nitrosyl complexes exhibit unusual chemical properties [18–21].

We have reported a convenient synthesis of the η^3 -allyl molybdenum and tungsten complexes with S_2CPR_3 ligands, $[MBr(CO)_2(\eta^3-C_3H_5)(S_2CPR_3)]$ ($M = Mo, W$), and their use as building blocks for bimetallic complexes with [22] or without [10] metal–metal bond. To extend this chemistry, mainly for comparative purposes, we have turned our attention now to the synthesis and reactivities of mono- and binuclear nitrosyl complexes containing S_2CPR_3 ligands. Herein we wish to report the preparation of a mononuclear nitrosyl complex $[MoBr(NO)(CO)_2(S_2CPCy_3)]$ (**3**), which is a useful precursor for the synthesis of binuclear complexes containing both NO and S_2CPR_3 ligands, such as $[(OC)_2(ON)Mo(\mu-S_2CPCy_3)(\mu-Br)M(CO)_3]$ (**4a**: $M = Mo$; **4b**: $M = W$). The displacement reactions of

* Corresponding author. Present address: Departamento de Química Inorgánica, Universidad de Valladolid, Real de Burgos/n, E-47071 Valladolid, Spain. Tel.: +34 83 423232; Fax: +34 83 423013; e-mail: dmsj@sauron.quimica.uniovi.es

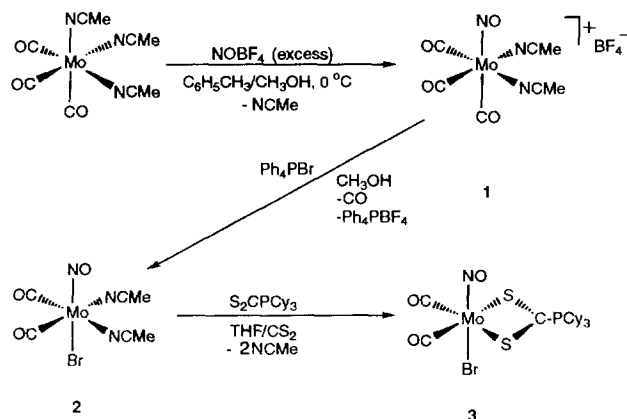
the binuclear complex **4a** with mono- and bidentate phosphine ligands are also described in this paper, as well as the X-ray crystal structure of $[(OC)_2(ON)Mo(\mu-Br)(\mu-S_2CPCy_3)Mo(CO)_2(PEt_3)]$ (**5a**). The new compounds **3** and **4** can be directly related to the previously reported $[MoBr(CO)_2(\eta^3-C_3H_5)(S_2CPCy_3)]$ and $[(\eta^3-C_3H_5)(CO)_2Mo(\mu-Br)(\mu-S_2CPCy_3)Mo(CO)_3]$, which contain the isoelectronic η^3 -allyl ligands instead of nitrosyl, and thus permit a direct comparison between the two series of isoelectronic compounds.

The coordination of the strong π -acceptor nitrosyl ligand should result in the decrease of the electron density at the metal center and even at the central carbon atom of the coordinated S_2CPCy_3 ligand, thus increasing the electronic asymmetry of the binuclear molecule. Therefore, it can be expected that the nitrosyl complexes may have some reactivity substantially different to that of their allyl analogs.

2. Results and discussion

The mononuclear nitrosyl complex **3** was prepared in three steps as summarized in Scheme 1.

Treatment of freshly prepared $[Mo(CO)_3(NCMe)_3]$ with an excess of $NOBF_4$ in a $C_6H_5CH_3/CH_3OH$ mixture at $0^\circ C$ led to a brown-yellow solution of the nitrosyl containing cation $[Mo(NO)(CO)_3(NCMe)_2]BF_4$ (**1**). Addition of bromide ion produces the neutral bromo complex $[MoBr(NO)(CO)_2(NCMe)_2]$ (**2**). Both Ph_4PBr and Et_4NBr can be used as a brominating agent for this



Scheme 1.

step, but the use of Ph_4PBr leads to a more straightforward workup since the salt Ph_4PBF_4 formed in the reaction is readily precipitated from the solution, thus avoiding additional workup. These first two steps were made in one pot. The intermediates **1** and **2** were characterized by IR spectroscopy in situ (in MeOH). Complex **1** shows two strong $\nu(CO)$ bands at 2029, and 1935 cm^{-1} ; and one band attributed to N–O stretching at 1680 cm^{-1} . The neutral bromo complex **2** displays the same pattern shifted, as expected, to lower frequencies [$\nu(CO)$: 2021, and 1926 cm^{-1} ; $\nu(NO)$: 1653 cm^{-1}].

When the adduct S_2CPCy_3 was added to a solution of **2** in THF, containing 1–2 ml (excess) of carbon disulfide, the novel nitrosyl complex $[MoBr(NO)(CO)_2(S_2CPCy_3)]$ (**3**) precipitated gradually from the solution

Table 1
IR and $^{31}P\{^1H\}$ -NMR data for the novel nitrosyl complexes

No.	Compound	IR (THF), cm^{-1}		$^{31}P\{^1H\}$ -NMR ^a , δ (ppm)		
		$\nu(CO)$	$\nu(NO)$	(S_2CP)	Mo^0-P	Mo^+-P
3	$[Mo(NO)(CO)_2(S_2CPCy_3)Br]$	2019s, 1922vs	1645s	29.41		
4a	$[(OC)_2(ON)Mo(\mu-S_2CPCy_3)(\mu-Br)Mo(CO)_3]$	2034m, 2017s 1953vs, 1867s	1647s	37.26		
4b	$[(OC)_2(ON)Mo(\mu-S_2CPCy_3)(\mu-Br)W(CO)_3]$	2033s, 2013vs, 1953vs 1934s, 1863s	1650s	35.38		
5a	$[(OC)_2(ON)Mo(\mu-S_2CPCy_3)(\mu-Br)Mo(CO)_2(PEt_3)]$	2020m, 1941s 1921s, 1807m	1639s	36.28	27.15	
5b	$[(OC)_2(ON)Mo(\mu-S_2CPCy_3)(\mu-Br)Mo(CO)_2P(OMe)_3]$	2022m, 1942vs, 1833s	1641s	36.70	133.88 ^b	
6a	$[(OC)_2(ON)Mo(\mu-S_2CPCy_3)(\mu-Br)(\mu-dppm)Mo(CO)_2]$	2029s, 1950s 1913vs, 1778m	1642s	40.14	11.80d ($J_{p-p} = 18\text{ Hz}$)	7.56d ^b
6b	$[(OC)_2(ON)Mo(\mu-S_2CPCy_3)(\mu-Br)(\mu-dppm)Mo(CO)_2]$	2030s, 1960s 1919vs, 1784m	1641s	40.44	35.39d ($J_{p-p} = 31\text{ Hz}$)	13.33d ^b

^a In $CDCl_3$ unless otherwise stated. Mo^+ denotes the atom bearing the nitrosyl ligand.

^b In CD_2Cl_2 .

as a brown crystalline solid. In the solid state, complex **3** can be handled in air for a short time and its solubility, even in THF or CH_2Cl_2 , is rather low. When a solution of **3** was exposed to air or heated, especially in CH_2Cl_2 or CHCl_3 , the nitrosyl complex was decomposed within minutes, thus being much less stable than its allyl analog $[\text{MoBr}(\text{CO})_2(\eta^3\text{-C}_3\text{H}_5)(\text{S}_2\text{CPR}_3)]$ [22].

Complex **3** has been characterized by IR, ^1H - and ^{31}P -NMR spectroscopy (Tables 1 and 2) and elemental analysis (see Section 3). The carbonyl ligands of **3** display two strong bands in the IR spectrum at 2028 and 1948 cm^{-1} (in CH_2Cl_2). The strong band at 1641 cm^{-1} is attributed to the N–O stretching vibration of the coordinated nitrosyl ligand. Although it is difficult to diagnose linear and bent M–NO modes for nitrosyl transition metal complexes by simply using measured values of $\nu(\text{NO})$, the empirical rules advanced by Ibers and his co-workers are useful in distinguishing the two bonding modes of nitrosyl ligands [23,24]. According to

these rules, the corrected value of $\nu(\text{NO})$ for **3** is 1731 cm^{-1} , which suggests a linear Mo–N–O structure. The $^{31}\text{P}\{^1\text{H}\}$ -NMR spectrum consists of a unique singlet signal at δ 29.4 ppm (CDCl_3). The spectroscopic data indicate that the complex **3** is formed as the only detectable product. When compared with the η^3 -allyl complex $[\text{MoBr}(\text{CO})_2(\eta^3\text{-C}_3\text{H}_5)(\text{S}_2\text{CPCy}_3)]$ ($\nu(\text{CO})$ 1941, 1860 cm^{-1} , in CH_2Cl_2), the $\nu(\text{CO})$ bands of **3** move to much higher frequency, reflecting the strong electron withdrawing effect of the NO ligand. Since in the complex **3** there are three good π -electron-accepting ligands, two carbonyls and one nitrosyl ligand, the Mo atom of **3** is expected to be very electron deficient, and not suitable to release electron density through back-donation. We have shown in previous papers [10,15,22,25] that the phosphonodithioformate ligand bind a metal fragment in a η^3 -(S,C,S') bonding mode when the metal is enough electron-rich to back-donate electron density to the central carbon of the ligand. On

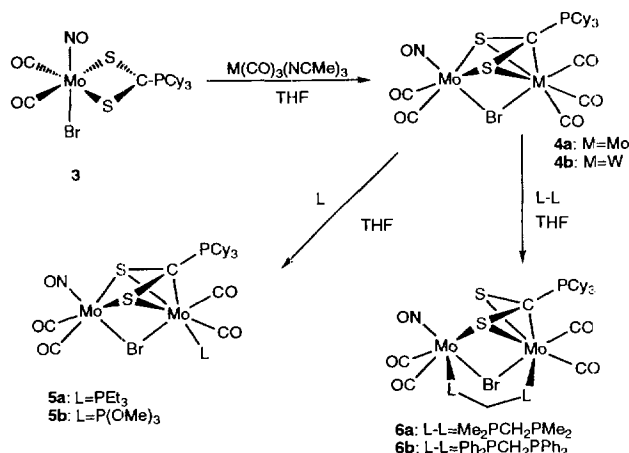
Table 2
 ^1H - and $^{13}\text{C}\{^1\text{H}\}$ -NMR data for the novel nitrosyl complexes

Compound	^1H -NMR, δ , ppm	$^{13}\text{C}\{^1\text{H}\}$ -NMR, δ , ppm
3 ^a	2.50 [m, 3 H, CH of Cy], 2.02 ~ 1.35 [m, br., 30 H, CH ₂ of Cy]	
4a ^a	2.63 [m, 3 H, CH of Cy], 1.95 ~ 1.26 [m, br., 30 H, CH ₂ of Cy]	241.6 [d(6), 2 Mo ⁰ CO], 217.0 [s, Mo ⁰ CO], 216.5 [s, 2 Mo ⁺ CO], 104.1 [d(38), S ₂ CP], 33.2 [d(39), C ¹ of Cy], 27.4 [s, C ² and C ⁶ of Cy], 26.7 [d(12), C ³ and C ⁵ of Cy], 25.2 [s, C ⁴ of Cy]
4b ^a	2.56 [m, 3 H, CH of Cy], 1.95 ~ 1.27 [m, br., 30 H, CH ₂ of Cy]	233.1 [d(6), 2 WCO], 216.3 [s, WCO], 215.0 [s, 2 Mo ⁺ CO], 93.5 [d(41), S ₂ CP], 33.3 [d(39), C ¹ of Cy], 27.4 [s, C ² and C ⁶ of Cy], 26.7 [d(12), C ³ and C ⁵ of Cy], 25.3 [s, C ⁴ of Cy]
5a ^a	2.61 [m, 3 H, CH of Cy], 2.04 ~ 1.11 [m, br., 45 H, P(CH ₂ CH ₃) and CH ₂ of Cy]	253.6 [dd(22 and 7), Mo ⁰ CO], 231.3 [d(5), Mo ⁰ CO], 218.5 [s, Mo ⁺ CO], 216.4 [s, Mo ⁺ CO], 96.8 [dd(41 and 4), S ₂ CP], 33.2 [d(44), C ¹ of Cy], 27.4 [s, br., C ² and C ⁶ of Cy], 26.8 [d(11), C ³ and C ⁵ of Cy], 25.4 [s, C ⁴ of Cy], 18.3 [d(23), CH ₂ of PEt ₃], 7.7 [s, CH ₃ of PEt ₃]
5b ^b	3.72 [d(11), 9 H, POCH ₃], 2.62 [m, 3 H, CH of Cy], 1.91 ~ 1.35 [m, br., 30 H, CH ₂ of Cy]	248.5 [m, br., Mo ⁰ CO], 229.9 [d(8), Mo ⁰ CO], 218.7 [s, Mo ⁺ CO], 217.1 [s, Mo ⁺ CO], 99.9 [dd(40 and 5), S ₂ CP], 52.7 [s, POCH ₃], 33.4 [d(42), C ¹ of Cy], 27.6 [s, C ² and C ⁶ of Cy], 27.2 [d(11), C ³ and C ⁵ of Cy], 25.8 [s, C ⁴ of Cy]
6a ^b	3.03 [m, 1 H, PCH ₂ P of dmpm], 2.63 [m, 4 H, CH of Cy and PCH ₂ P of dmpm], 2.02 ~ 1.28 [m, br., 42 H, CH ₂ of Cy and PCH ₃ of dmpm]	246.8 [dd(18 and 5), Mo ⁰ CO], 230.2 [d(8), Mo ⁰ CO], 212.8 [d(31), Mo ⁺ CO], 208.8 [d(8), Mo ⁺ CO], 78.7 [ddd(58,14 and 7), S ₂ CP], 39.1 [dd(16 and 8), PCH ₂ P of dmpm], 33.9 [d(41), C ¹ of Cy], 27.5 [s, C ² and C ⁶ of Cy], 27.4 [d(12), C ³ and C ⁵ of Cy], 25.9 [s, C ⁴ of Cy], 20.5–18.7 [m, CH ₃ of dmpm]
6b ^b	7.98 ~ 6.95 [m, 20 H, C ₆ H ₅ of dppm], 4.71 [m, 1 H, PCH ₂ P of dppm], 3.82 [m, 1 H, PCH ₂ P of dppm], 2.68 [m, 3 H, CH of Cy], 2.22 ~ 1.32 [m, 30 H, CH ₂ of Cy]	247.9 [dd(17 and 5), Mo ⁰ CO], 229.2 [d(7), Mo ⁰ CO], 214.9 [d(56), Mo ⁺ CO], 212.4 [d(8), Mo ⁺ CO], 140.2 [dd(36 and 8), C ¹ of Ph], 138.5 [dd(37 and 8), C ¹ of Ph], 135.6–128.2 [m, CH of Ph], 78.6 [ddd(61,10 and 4), S ₂ CP], 35.2 [d(39), C ¹ of Cy], 32.5 [dd(14 and 10), PCH ₂ P of dppm], 28.4 [dd(34 and 3), C ² and C ⁶ of Cy], 27.5 [d(12), C ³ and C ⁵ of Cy], 26.2 [s, C ⁴ of Cy]

^a In CDCl_3 .

^b In CD_2Cl_2 .

Coupling constants in parentheses are in Hz.



Scheme 2.

the other hand, when the ligand is bonded to a electron-poor metal-ligand fragment, the $\eta^2(\text{S},\text{S}')$ chelate bonding mode is preferred. According to this, the structure which has been tentatively proposed for **3** in Scheme 1, contains the S_2CPR_3 acting as chelate. ^{13}C -NMR data could be of great help in this regard but, unfortunately, the attempts to acquire good ^{13}C -NMR spectra for the mononuclear nitrosyl complex **3** were thwarted by its limited solubility. Additional support for the structure proposed for **3** is given by the structure determination of the derivative **5a** (see below).

Compound **3** reacts smoothly with $\text{M}(\text{CO})_3(\text{NCR})_3$ ($\text{M} = \text{Mo}$, $\text{R} = \text{Me}$; $\text{M} = \text{W}$, $\text{R} = \text{Et}$) in THF at room temperature to afford new nitrosyl binuclear complexes $[(\text{OC})_2(\text{ON})\text{Mo}(\mu\text{-Br})(\mu\text{-S}_2\text{CPCy}_3)\text{M}(\text{CO})_3]$ (**4a**: $\text{M} = \text{Mo}$; **4b**: $\text{M} = \text{W}$) which can be isolated as red crystals in 85–90% yields (Scheme 2). In the solid state, complexes **4a–b** can be handled in air for several hours. However, they are gradually decomposed in solution especially in chlorinated solvents, even under dry nitrogen atmosphere.

Complexes **4a** and **4b** were characterized by IR, ^1H -, ^{31}P - and ^{13}C -NMR spectra (Tables 1 and 2) and elemental analysis (see Section 3). The binuclear nitrosyl pentacarbonyl complex **4a** displays four $\nu(\text{CO})$ bands at 2034m, 2017s, 1953vs, and 1867s cm^{-1} (in CH_2Cl_2), while **4b** exhibits five $\nu(\text{CO})$ bands at 2033s, 2013vs, 1953vs, 1934s, and 1863s, cm^{-1} . A comparison of the spectra of both compounds suggests that in the spectrum of **4a** there is an accidental coincidence of two normal modes to give a single, broad band at 1953 cm^{-1} , which is split into two bands (1953vs and 1934s cm^{-1}) for the tungsten derivative **4b**. In both compounds the $\nu(\text{CO})$ bands move to higher energies when compared with those of their analog $[(\eta^3\text{-C}_3\text{H}_5)(\text{OC})_2\text{Mo}(\mu\text{-Br})(\mu\text{-S}_2\text{CPCy}_3)\text{Mo}(\text{CO})_3]$ which appear in the range 2023–1856 cm^{-1} [22]. The $\nu(\text{NO})$ absorption of **4a** appears at 1643 cm^{-1} (1646 cm^{-1} for **4b**) close to that of the starting compound **3**. Only one singlet signal is

observed in the $^{31}\text{P}\{^1\text{H}\}$ -NMR spectra of **4a** (at δ 37.3) or **4b** (at δ 35.4 ppm). In the $^{13}\text{C}\{^1\text{H}\}$ -NMR spectrum of **4a** (CDCl_3 solution) the signal of the central carbon of the S_2CPCy_3 ligand rises at δ 104.1 ppm as a doublet with $^1J(\text{P-C}) = 38$ Hz. This signal is shifted markedly downfield compared with its η^3 -allyl binuclear analog (δ 90.5 ppm, CDCl_3) [22]. This shift can be attributed to the π -accepting ability of the NO ligand. The same effect is observed in the signals of the tungsten derivatives (δ 93.5 ppm for **4b**, compared to δ 80.8 ppm for the corresponding allyl derivative [22]). The good ability of nitrosyl ligand to accommodate electron density via back-donation from the metal is reflected in the IR spectra of the complexes. Thus, the $\nu(\text{NO})$ absorption of the free NO at 1876 cm^{-1} [26] is shifted to much lower frequencies (1640–1650 cm^{-1}) for NO ligands coordinated to Mo atoms in complexes **3** and **4**. It can be anticipated that the Mo atom bonded to nitrosyl, and the central carbon atom of the S_2CPR_3 ligand are more electron deficient in the complexes **3** and **4**, than the corresponding atoms in their allyl analogs. Therefore, the nucleophilic hydride addition to the central carbon atoms of S_2CPR_3 ligands might be more favorable and the coordination of the central carbon of the S_2CPCy_3 ligand to the Mo center of the 'Mo(NO)(CO)₂' fragments should be even less favorable than in the 'Mo(CO)₂($\eta^3\text{-C}_3\text{H}_5$)' case. These predictions are consistent with our recent experimental results which will be published when completed.

The reactivity of the pentacarbonyl nitrosyl complex **4a** towards mono- and bidentate phosphine ligands is

Table 3
Crystallographic data for $[(\text{OC})_2(\text{ON})\text{Mo}(\mu\text{-Br})(\mu\text{-S}_2\text{CPCy}_3)\text{Mo}(\text{CO})_2(\text{PEt}_3)]$ (**5a**)

Formula	$\text{C}_{29}\text{H}_{48}\text{BrMo}_2\text{NO}_5\text{P}_2\text{S}_2$
fw	884.6
Crystal size, mm; color	parallelepiped; dark red
Crystal system, space group	orthorhombic, $\text{P}c a n$
a , Å	15.214(13)
b , Å	22.825(8)
c , Å	42.284(12)
V , Å ³	14683(22)
Z	16
Temp., K	293
ρ_{calc} , g cm^{-3}	1.61
$F(000)$	7200
λ (Mo $\text{K}\alpha$), Å	0.71069
μ , cm^{-1}	19.75
Scan range, deg	$1 \leq \theta \leq 20$
h, k, l values	$0 \leq h \leq 14, 0 \leq k \leq 21, 0 \leq l \leq 40$
No. of reflections collected	6794
No. of reflections observed	1990 [$I \geq 3\sigma(I)$]
No. of parameters	338
Goodness of fit	1.43
Weighting scheme	units
Residuals ^a R, R_w	0.093, 0.096

^a $R = \Sigma(|F_o| - |F_c|) / \Sigma|F_o|$, $R_w = \{\Sigma(w(|F_o| - |F_c|)^2) / \Sigma w|F_o|^2\}^{1/2}$.

Table 4
Atomic coordinates and isotropic displacement coefficients (\AA^2) for
[[$(\text{OC})_2(\text{ON})\text{Mo}(\mu\text{-Br})(\mu\text{-S}_2\text{CPCy}_3)\text{Mo}(\text{CO})_2(\text{PEt}_3)_3$)] (**5a**)

Atom	x/a	y/b	z/c	$U(\text{iso})$
MOLECULE 1				
Mo(1)	0.0200(3)	0.1594(2)	0.3429(1)	0.053(1)
Mo(2)	0.0171(3)	0.1370(2)	0.4219(1)	0.041(1)
Br(1)	-0.0057(4)	0.2396(3)	0.3895(2)	0.080(2)
S(1)	0.1241(9)	0.1025(7)	0.3796(4)	0.057(4)
S(2)	-0.0688(9)	0.0884(7)	0.3782(4)	0.053(4)
P(1)	0.128(1)	0.1964(8)	0.4499(4)	0.067(5)
P(2)	0.0412(9)	-0.0183(6)	0.3981(4)	0.045(4)
O(1)	0.037(4)	0.092(2)	0.286(1)	0.12(2)
O(2)	0.155(3)	0.250(2)	0.315(1)	0.08(1)
O(3)	-0.133(3)	0.226(2)	0.305(1)	0.10(2)
O(4)	0.029(2)	0.066(2)	0.483(1)	0.07(1)
O(5)	-0.157(3)	0.157(2)	0.459(1)	0.08(1)
C(1)	0.032(3)	0.056(2)	0.394(1)	0.03(1)
X(1) ^a	0.033(4)	0.114(2)	0.309(1)	0.07(2)
X(2) ^a	0.104(5)	0.217(3)	0.327(2)	0.11(3)
X(3) ^a	-0.075(4)	0.202(3)	0.320(2)	0.09(2)
C(4)	0.025(3)	0.089(2)	0.458(1)	0.04(1)
C(5)	-0.091(3)	0.147(2)	0.447(1)	0.04(1)
C(6)	0.186(5)	0.255(4)	0.429(2)	0.10(2)
C(7)	0.251(7)	0.225(4)	0.406(3)	0.18(4)
C(8)	0.209(4)	0.150(3)	0.470(2)	0.09(2)
C(9)	0.287(4)	0.192(3)	0.486(2)	0.08(2)
C(10)	0.085(5)	0.260(4)	0.476(2)	0.12(3)
C(11)	0.021(6)	0.234(4)	0.500(2)	0.15(3)
C(20)	0.071(3)	-0.052(2)	0.361(1)	0.04(2)
C(21)	0.173(4)	-0.039(3)	0.351(2)	0.08(2)
C(22)	0.192(4)	-0.077(3)	0.320(2)	0.07(2)
C(23)	0.130(5)	-0.057(4)	0.294(2)	0.11(3)
C(24)	0.036(4)	-0.072(2)	0.304(1)	0.06(2)
C(25)	0.011(3)	-0.033(2)	0.333(1)	0.04(1)
C(30)	0.113(4)	-0.036(3)	0.430(1)	0.06(2)
C(31)	0.199(4)	-0.000(3)	0.432(2)	0.07(2)
C(32)	0.244(4)	-0.013(3)	0.464(2)	0.09(2)
C(33)	0.269(4)	-0.077(3)	0.464(1)	0.06(2)
C(34)	0.185(4)	-0.114(3)	0.464(2)	0.08(2)
C(35)	0.137(4)	-0.103(3)	0.432(2)	0.07(2)
C(40)	-0.065(4)	-0.044(2)	0.407(1)	0.06(2)
C(41)	-0.077(4)	-0.112(3)	0.399(2)	0.08(2)
C(42)	-0.178(4)	-0.126(3)	0.402(2)	0.07(2)
C(43)	-0.207(4)	-0.115(3)	0.436(2)	0.08(2)
C(44)	-0.197(5)	-0.049(3)	0.442(2)	0.10(2)
C(45)	-0.099(3)	-0.034(2)	0.441(1)	0.04(1)
MOLECULE 2				
Mo(51)	0.4894(3)	-0.1582(2)	0.4062(1)	0.046(1)
Mo(52)	0.5091(3)	-0.1363(2)	0.3263(1)	0.039(1)
Br(51)	0.4700(4)	-0.2367(3)	0.3584(2)	0.082(2)
S(51)	0.6001(8)	-0.1037(6)	0.3738(3)	0.036(4)
S(52)	0.4133(9)	-0.0891(6)	0.3675(3)	0.042(4)
P(51)	0.633(1)	-0.1963(7)	0.3020(4)	0.059(5)
P(52)	0.529(1)	0.0165(7)	0.3495(4)	0.052(4)
O(51)	0.502(3)	-0.086(2)	0.465(1)	0.08(1)
O(52)	0.615(4)	-0.241(3)	0.438(1)	0.15(2)
O(53)	0.329(3)	-0.223(2)	0.435(1)	0.10(2)
O(55)	0.350(2)	-0.155(2)	0.2816(9)	0.06(1)
O(54)	0.555(2)	-0.066(2)	0.2675(9)	0.06(1)
C(51)	0.518(4)	-0.064(3)	0.356(1)	0.07(2)
X(51) ^a	0.500(3)	-0.117(2)	0.441(1)	0.04(1)
X(52) ^a	0.562(5)	-0.217(3)	0.425(2)	0.10(2)
X(53) ^a	0.392(3)	-0.198(2)	0.427(1)	0.05(2)

Table 4 (continued)

Atom	x/a	y/b	z/c	$U(\text{iso})$
MOLECULE 2				
C(55)	0.412(4)	-0.151(3)	0.300(2)	0.07(2)
C(54)	0.537(4)	-0.096(2)	0.291(1)	0.05(2)
C(56)	0.672(5)	-0.267(4)	0.322(2)	0.12(3)
C(57)	0.719(4)	-0.252(3)	0.352(1)	0.06(2)
C(58)	0.732(3)	-0.152(2)	0.298(1)	0.05(2)
C(59)	0.810(4)	-0.193(3)	0.286(2)	0.08(2)
C(60)	0.602(4)	-0.222(3)	0.261(1)	0.07(2)
C(61)	0.530(4)	-0.267(2)	0.260(1)	0.06(2)
C(70)	0.620(4)	0.036(3)	0.323(2)	0.07(2)
C(71)	0.704(4)	-0.005(3)	0.327(2)	0.09(2)
C(72)	0.765(4)	0.007(3)	0.298(2)	0.06(2)
C(73)	0.793(4)	0.073(3)	0.299(2)	0.09(2)
C(74)	0.712(4)	0.109(3)	0.294(2)	0.06(2)
C(75)	0.651(3)	0.100(2)	0.323(1)	0.04(1)
C(80)	0.424(4)	0.046(3)	0.333(2)	0.07(2)
C(81)	0.413(3)	0.113(2)	0.340(1)	0.05(2)
C(82)	0.320(3)	0.130(2)	0.331(1)	0.05(2)
C(83)	0.311(4)	0.122(3)	0.295(2)	0.07(2)
C(84)	0.322(4)	0.056(3)	0.288(1)	0.06(2)
C(85)	0.416(5)	0.038(3)	0.298(2)	0.10(3)
C(90)	0.545(4)	0.057(3)	0.389(1)	0.07(2)
C(91)	0.468(5)	0.044(3)	0.411(2)	0.09(2)
C(92)	0.477(4)	0.083(3)	0.440(2)	0.09(2)
C(93)	0.557(5)	0.063(3)	0.458(2)	0.09(2)
C(94)	0.640(5)	0.075(4)	0.438(2)	0.12(3)
C(95)	0.630(4)	0.037(3)	0.405(2)	0.09(2)

^a Atoms X are 1/3 nitrogen, 2/3 carbon.

similar to that found for the hexacarbonyl complexes $[(\text{OC})_3\text{M}(\mu\text{-Br})(\mu\text{-S}_2\text{CPR}_3)\text{Mo}(\text{CO})_3]$ ($\text{M} = \text{Mn}, \text{Re}$), which have been reported previously [27,28]. Complex **4a** reacted instantaneously with monodentate phosphine or phosphite ligands in THF at room temperature to afford a deep red solution, from which red brown crystals of $[(\text{OC})_2(\text{ON})\text{Mo}(\mu\text{-Br})(\mu\text{-S}_2\text{PCy}_3)\text{Mo}(\text{CO})_2(\text{L})]$ (**5a**, $\text{L} = \text{PEt}_3$; **5b**, $\text{L} = \text{P}(\text{OMe})_3$) were isolated in almost quantitative yields (Scheme 2). As found in our previous studies, potentially bidentate phosphine ligands $\text{R}_2\text{PCH}_2\text{PR}_2$ replace one carbonyl ligand from the 'Mo(CO)₃' fragment, and one of the sulfur bridges from the 'Mo(CO)₂(NO)' fragment to give complexes $[(\text{OC})_2(\text{ON})\text{Mo}(\mu\text{-Br})(\mu\text{-S}_2\text{CPCy}_3)(\mu\text{-L-L})\text{Mo}(\text{CO})_2]$ (**6a**: $\text{L-L} = \text{Me}_2\text{PCH}_2\text{PMe}_2$; **6b**: $\text{L-L} = \text{Ph}_2\text{PCH}_2\text{PPh}_2$). These can be isolated as red brown microcrystals in moderate yields. The complex with dppm (**6b**) is more stable than the complex with dmpm (**6a**), whereas their analogs $[(\text{OC})_3\text{M}(\mu\text{-Br})(\mu\text{-S}_2\text{CPCy}_3)(\mu\text{-L-L})\text{Mo}(\text{CO})_2]$ ($\text{M} = \text{Mn}, \text{Re}$) show the opposite relative stability. Complex **6a** gradually decomposed in solution at room temperature, even under dry nitrogen atmosphere, while the IR spectrum of a solution of **6b** in THF showed no noticeable change after stirring at room temperature for 2 days. Both **6a** and **6b** are thermally unstable in solution and decompose quickly when heated in solution. The formation of the derivatives **5** and **6** by substitution reactions from **4**,

Table 5

Selected bond lengths (Å) and angles (°) for $[(OC)_2(ON)Mo(\mu-Br)(\mu-S_2CPCy_3)Mo(CO)_2(PEt_3)]$ (5a)

MOLECULE 1			
Mo(1)–Br(1)	2.719(9)	Mo(1)–S(1)	2.57(2)
Mo(1)–S(2)	2.59(2)	Mo(1)–X(1)	1.76(6)
Mo(1)–X(2)	1.96(8)	Mo(1)–X(3)	1.99(7)
Mo(2)–Br(1)	2.735(8)	Mo(2)–S(1)	2.54(2)
Mo(2)–S(2)	2.52(2)	Mo(2)–P(1)	2.47(2)
Mo(2)–C(1)	2.20(4)	Mo(2)–C(4)	1.87(5)
Mo(2)–C(5)	1.96(5)		
S(1)–C(1)	1.87(5)	S(2)–C(1)	1.83(4)
P(1)–C(6)	1.83(8)	P(1)–C(8)	1.82(7)
P(1)–C(10)	1.96(8)	P(2)–C(1)	1.71(5)
P(2)–C(20)	1.79(5)	P(2)–C(30)	1.78(6)
P(2)–C(40)	1.77(6)	O(1)–X(1)	1.10(7)
O(2)–X(2)	1.19(7)	O(3)–X(3)	1.22(7)
O(4)–C(4)	1.18(5)	O(5)–C(5)	1.14(5)
Br(1)–Mo(1)–S(1)	89.4(4)	Br(1)–Mo(1)–S(2)	85.8(4)
S(1)–Mo(1)–S(2)	69.9(5)	Br(1)–Mo(1)–X(1)	173.1(18)
S(1)–Mo(1)–X(1)	97.0(18)	S(2)–Mo(1)–X(1)	98.8(18)
Br(1)–Mo(1)–X(2)	84.1(22)	S(1)–Mo(1)–X(2)	98.5(21)
S(2)–Mo(1)–X(2)	164.7(22)	X(1)–Mo(1)–X(2)	92.3(28)
Br(1)–Mo(1)–X(3)	85.6(19)	S(1)–Mo(1)–X(3)	170.8(19)
S(2)–Mo(1)–X(3)	102.0(18)	X(1)–Mo(1)–X(3)	88.4(26)
X(2)–Mo(1)–X(3)	88.6(26)	Br(1)–Mo(1)–X(3)	85.6(19)
S(1)–Mo(1)–X(3)	170.8(19)	S(2)–Mo(1)–X(3)	102.0(18)
Br(1)–Mo(2)–S(1)	89.6(4)	Br(1)–Mo(2)–S(2)	86.8(4)
S(1)–Mo(2)–S(2)	71.4(5)	Br(1)–Mo(2)–P(1)	81.7(5)
S(1)–Mo(2)–P(1)	93.9(6)	S(2)–Mo(2)–P(1)	161.4(6)
Br(1)–Mo(2)–C(1)	117.7(12)	S(1)–Mo(2)–C(1)	45.6(12)
S(2)–Mo(2)–C(1)	44.9(11)	P(1)–Mo(2)–C(1)	130.3(12)
Br(1)–Mo(2)–C(4)	156.4(15)	S(1)–Mo(2)–C(4)	110.0(15)
S(2)–Mo(2)–C(4)	111.5(15)	P(1)–Mo(2)–C(4)	83.8(15)
C(1)–Mo(2)–C(4)	85.9(19)	Br(1)–Mo(2)–C(5)	93.9(15)
S(1)–Mo(2)–C(5)	161.3(15)	S(2)–Mo(2)–C(5)	90.5(15)
P(1)–Mo(2)–C(5)	104.8(15)	C(1)–Mo(2)–C(5)	117.6(19)
C(4)–Mo(2)–C(5)	71.9(20)	Mo(1)–Br(1)–Mo(2)	76.6(2)
Mo(1)–S(1)–Mo(2)	82.8(5)	Mo(1)–S(1)–C(1)	91.3(14)
Mo(2)–S(1)–C(1)	57.6(14)	Mo(1)–S(2)–Mo(2)	82.9(5)
Mo(1)–S(2)–C(1)	91.7(15)	Mo(2)–S(2)–C(1)	58.3(14)
Mo(1)–X(1)–O(1)	170.5(59)	Mo(2)–C(1)–S(1)	76.8(16)
Mo(2)–C(1)–S(2)	76.8(16)	S(1)–C(1)–S(2)	106.1(22)
Mo(2)–C(1)–P(2)	142.1(26)	S(1)–C(1)–P(2)	122.4(25)
S(2)–C(1)–P(2)	120.5(25)	Mo(1)–X(2)–O(2)	175.9(65)
Mo(1)–X(3)–O(3)	177.2(59)	Mo(2)–C(4)–O(4)	169.3(43)
Mo(2)–C(5)–O(5)	172.3(47)	P(1)–C(6)–C(7)	107.4(62)
MOLECULE 2			
Mo(51)–Br(51)	2.718(9)	Mo(51)–S(51)	2.50(1)
Mo(51)–S(52)	2.55(1)	Mo(51)–X(51)	1.77(5)
Mo(51)–X(52)	1.91(7)	Mo(51)–X(53)	1.95(5)
Mo(52)–Br(51)	2.729(9)	Mo(52)–S(51)	2.55(1)
Mo(52)–S(52)	2.51(1)	Mo(52)–P(51)	2.55(2)
Mo(52)–C(51)	2.09(6)	Mo(52)–C(55)	1.89(6)
Mo(52)–C(54)	1.82(6)		
S(51)–C(51)	1.72(6)	S(52)–C(51)	1.76(6)
P(51)–C(56)	1.91(8)	P(51)–C(58)	1.82(5)
P(51)–C(60)	1.90(6)	P(52)–C(51)	1.86(6)
P(52)–C(70)	1.83(6)	P(52)–C(80)	1.87(6)
P(52)–C(90)	1.92(6)	O(51)–X(51)	1.22(5)
O(52)–X(52)	1.12(8)	O(53)–X(53)	1.16(6)
O(55)–C(55)	1.22(6)	O(54)–C(54)	1.23(6)
Br(51)–Mo(51)–S(51)	89.6(4)	Br(51)–Mo(51)–S(52)	83.1(4)
S(51)–Mo(51)–S(52)	69.2(4)	Br(51)–Mo(51)–X(51)	171.1(14)
S(51)–Mo(51)–X(51)	97.5(14)	S(52)–Mo(51)–X(51)	104.4(14)

Table 5 (continued)

MOLECULE 2			
Br(51)–Mo(51)–X(52)	85.2(22)	S(51)–Mo(51)–X(52)	101.0(21)
S(52)–Mo(51)–X(52)	164.8(22)	X(51)–Mo(51)–X(52)	88.2(26)
Br(51)–Mo(51)–X(53)	86.5(16)	S(51)–Mo(51)–X(53)	171.8(16)
S(52)–Mo(51)–X(53)	103.0(15)	X(51)–Mo(51)–X(53)	87.0(21)
X(52)–Mo(51)–X(53)	85.9(24)	Br(51)–Mo(52)–S(51)	88.4(4)
Br(51)–Mo(52)–S(52)	83.6(4)	S(51)–Mo(52)–S(52)	69.2(4)
Br(51)–Mo(52)–P(51)	84.9(4)	S(51)–Mo(52)–P(51)	94.1(5)
S(52)–Mo(52)–P(51)	159.9(5)	Br(51)–Mo(52)–C(51)	112.4(16)
S(51)–Mo(52)–C(51)	41.9(16)	S(52)–Mo(52)–C(51)	43.9(16)
P(51)–Mo(52)–C(51)	128.4(16)	Br(51)–Mo(52)–C(55)	88.5(19)
S(51)–Mo(52)–C(55)	161.1(19)	S(52)–Mo(52)–C(55)	91.9(19)
P(51)–Mo(52)–C(55)	104.2(19)	C(51)–Mo(52)–C(55)	123.6(24)
Br(51)–Mo(52)–C(54)	152.4(17)	S(51)–Mo(52)–C(54)	112.4(18)
S(52)–Mo(52)–C(54)	119.9(17)	P(51)–Mo(52)–C(54)	76.0(18)
C(51)–Mo(52)–C(54)	95.2(24)	C(55)–Mo(52)–C(54)	77.3(25)
Mo(51)–Br(51)–Mo(52)	78.0(2)	Mo(51)–S(51)–Mo(52)	85.4(4)
Mo(51)–S(51)–C(51)	90.8(2)	Mo(52)–S(51)–C(51)	54.4(20)
Mo(51)–S(52)–Mo(52)	85.2(4)	Mo(51)–S(52)–C(51)	88.1(19)
Mo(52)–S(52)–C(51)	55.1(19)	Mo(51)–X(51)–O(51)	176.2(42)
Mo(52)–C(51)–S(51)	83.7(24)	Mo(52)–C(51)–S(52)	81.0(23)
S(51)–C(51)–S(52)	111.4(32)	Mo(52)–C(51)–P(52)	134.1(33)
S(51)–C(51)–P(52)	121.5(32)	S(52)–C(51)–P(52)	116.4(31)
Mo(51)–X(52)–O(52)	164.7(72)	Mo(51)–X(53)–O(53)	171.5(51)
Mo(52)–C(55)–O(55)	173.9(54)	Mo(52)–C(54)–O(54)	175.2(48)

differs markedly from the behavior of its allyl analog, $[(\eta^3\text{-C}_3\text{H}_5)(\text{OC})_2\text{Mo}(\mu\text{-Br})(\mu\text{-S}_2\text{CPCy}_3)\text{Mo}(\text{CO})_3]$ which, when treated with PR_3 ($\text{R} = \text{Et}, \text{OMe}$) or $\text{R}_2\text{PCH}_2\text{PR}_2$ ($\text{R} = \text{Me}, \text{Ph}$) produced extensive decomposition [29]. Since the spectroscopic and X-ray data show the close similarity of the structures of the 'Mo(CO)₃' fragments in both nitrosyl and allyl complexes, the only rational explanation for the different reactivity of **4a** and its allyl analog is that PR_3 may attack on the allyl ligand, leading to loss of the allyl and resulting in decomposition. Some precedents have been reported for this behavior, such as the reactions of $[\text{MoCl}(\text{CO})_2(\text{NCMe})_2(\eta^3\text{-C}_3\text{H}_5)]$ with PR_3 [30].

The new complexes **5a–b** and **6a–b** were characterized by IR, ¹H-, ³¹P- and ¹³C-NMR spectroscopy (Tables 1 and 2) and elemental analysis (see Section 3). All experimental data available so far are consistent with the molecular structures proposed in Scheme 2. The $\nu(\text{NO})$ bands of **5a–b** and **6a–b**, in the range 1639–1643 cm^{-1} (in THF) are close to the $\nu(\text{NO})$ frequency of the starting complex **4a** (1647 cm^{-1} , in THF). Complexes **5a** and **5b** show two singlets in the ³¹P{¹H}-NMR spectra, which are in the similar region to those observed for their [MMo] ($\text{M} = \text{Mn}, \text{Re}$) analogs. In contrast, in the ³¹P{¹H}-NMR spectra of **6a** and **6b**, each spectrum consists of a singlet and two doublets, the chemical shifts for the phosphorus atom of the S₂CPCy₃ ligand and for the phosphorus bonded to the Mo⁰ atom are not significantly different from those of the [MMo] ($\text{M} = \text{Mn}, \text{Re}$) analogs, while the signals for the phosphorus bonded to Mo in the 'Mo(NO)(CO)₂' fragment are notably shifted upfield when compared with those of

the [MnMo] complexes and downfield compared with those of the [ReMo] complexes. It is not unexpected that chemical shifts for central carbon atoms of the S₂CPCy₃ ligands in the ¹³C{¹H}-NMR spectra of the new nitrosyl complexes **5** and **6** appear at higher frequencies in comparison with their analogs. The signals of CO ligands of the 'Mo(CO)₂PR₃' are placed in close proximity to those observed for the corresponding carbonyls of the [MMo] ($\text{M} = \text{Mn}, \text{Re}$) analogs, suggesting that the geometry of the 'Mo(CO)₂PR₃' fragment is similar in both series of complexes. The comparison of the spectra allows for a consistent assignment of the signals of the 'Mo(CO)₂(NO)' fragment.

In order to distinguish to which molybdenum is bonded the central carbon atom of the S₂CPCy₃ ligand, an X-ray structural determination was carried out on a crystal of the derivative **5a**. Crystallographic data are collected in Table 3.

Final atomic positional parameters are in Table 4, and selected bond distances and angles are given in Table 5. A perspective drawing of the structure is presented in Fig. 1. The results of the X-ray study show that the molecule of complex **5a**, consist of two fragments, 'Mo(NO)(CO)₂' and 'Mo(CO)₂(PET₃)', linked by a bromine and the (S,C,S') donor set of the S₂CPCy₃ ligand. As expected, the S₂CPCy₃ ligand acts as $\eta^2(\text{S},\text{S}')$ chelate towards the Mo atom of the 'Mo(NO)(CO)₂' fragment and as $\eta^3(\text{S},\text{C},\text{S}')$ pseudoallyl to the Mo atom of the fragment 'Mo(CO)₂(PET₃)'.

These results are consistent with our previous hypothesis that in both homo- and heterobinuclear complexes with S₂CPR₃ ligands the central carbon atom of

the S_2CPR_3 ligands prefers to bind the transition metal in the lower oxidation state [22]. Until now we have not found any exception to this hypothesis. It is customary to consider the nitrosyl ligand as cationic NO^+ , and therefore the conventional rules of electron counting assign oxidation number zero to both metals in binuclear derivatives **4**, **5**, and **6**. However, as it has been discussed above, the spectroscopic data strongly indicate that the Mo atom bearing the nitrosyl ligand behaves as electron poorer, when compared with the metals of the other fragments $M(CO)_3$ ($M = Mo, W$), or $Mo(CO)_2(L)$. Therefore, the bonding mode found in the structure of **5a** agrees well with our previous findings in this field, since the central carbon prefers to bind the electron-richer metal.

Despite the electronic difference between the two Mo atoms, the bromide bridge is placed quite symmetrically, at virtually the same distance from the two Mo atoms. This is in contrast to that observed for the allyl derivative, in which the bromine atom is placed significantly closer to the molybdenum which bears the allyl (cf. 2.681(1) vs. 2.801(1) Å). Unfortunately, in the fragment ' $Mo(CO)_2(NO)$ ', the positions of the nitrosyl ligand and the two carbonyls are disordered, and the atoms denoted by X in Fig. 1 have been refined as 2/3 carbon and 1/3 nitrogen. As a consequence of the disorder, the quality of the data was poor, and this precluded the anisotropic refinement of the atoms. Therefore, the standard deviations are high, and the comparison of the geometric parameters can only be done up to a limited extent. Nevertheless, the distances and angles within the core atoms of the molecule of **5a** are comparable to those found in previous structures. The overall geometry of the fragment ' $Mo(CO)_2(PEt_3)$ ' resembles that of the fragment ' $Mo(CO)_2(PCy_3)$ ' found

in the structure of $[(Bu)Cl_2Sn(\mu-Cl)(\mu-S_2CPCy_3)Mo(CO)_2(PCy_3)]$ [31]. In both structures, the phosphine is placed in *trans* to one of the sulfur atoms, this being due probably to the greater tendency of the CO to occupy one position *trans* to the bromide bridge.

3. Experimental section

All reactions and manipulations were carried out under nitrogen atmosphere by using Schlenk techniques. Solvents were freshly distilled under nitrogen according to standard methods before use. $Mo(CO)_6$, $W(CO)_6$, $NOBF_4$, Ph_4PBr , S_2CPCy_3 and other reagents were purchased and used without further purification. $[Mo(CO)_3(NCMe)_3]$ [32] and $[W(CO)_3(NCEt)_3]$ [33] were prepared according to the literature. Infrared spectra were recorded on a Perkin–Elmer Paragon 1000 FT–IR spectrophotometer. NMR spectra were recorded on a Bruker AC-300 instrument. The 1H and ^{13}C spectra are referenced to internal TMS and the ^{31}P spectra to external 85% H_3PO_4 . Elemental analyses were performed on a Perkin–Elmer 240B microanalyser.

3.1. Preparation of $[MoBr(NO)(CO)_2(S_2CPCy_3)]$ (**3**)

$NOBF_4$ (351 mg, 3.0 mmol) was added to a suspension of $[Mo(CO)_3(NCMe)_3]$ (3.0 mmol) in a toluene/methanol (25:4, v/v) mixture, which had been pre-cooled to 0°C (ice-bath). After the mixture was stirred at 0°C for 30 min, only a very small amount of solid was left in the yellow brown solution. Another portion of $NOBF_4$ (175 mg, 1.5 mmol, in 50% excess) was added and the mixture was stirred at 0°C for another 30 min. When all the solvent was removed in vacuo, $[Mo(NO)(CO)_3(NCMe)_2]BF_4$ (**1**) was obtained as a brown oil. IR (MeOH): $\nu(CO)$ 2029 s, 1935 s cm^{-1} ; $\nu(NO)$ 1680 s cm^{-1} .

$[Mo(NO)(CO)_3(NCMe)_2]BF_4$ (**1**) was redissolved in MeOH (40 ml) and then Ph_4PBr (1.26 g, 3.0 mmol) was added. A large amount of Ph_4PBF_4 precipitate appeared immediately. The mixture was stirred for 1 h. After removal of the methanol, THF (20 ml) was added. The yellow suspension was filtrated through kieselguhr and the filtrate was concentrated to ca. 20 ml. The IR spectrum shows the presence of $[MoBr(NO)(CO)_2(NCMe)_2]$ (**2**): $\nu(CO)$ 2021 s, 1926 s cm^{-1} ; $\nu(NO)$ 1646 s cm^{-1} .

Carbon disulfide (2 ml, in excess) and the adduct S_2CPCy_3 (1.06 g, 3.0 mmol) were added to the solution. The clear, yellow solution quickly turned to red brown and some red brown precipitate appeared. After the mixture was stirred for 2 h, hexane (10 ml) was added and the solution was removed out by a cannula filter. The brown crystalline solid (**3**) was washed with THF/hexane (2:1, v/v) and then dried in vacuo. Yield:

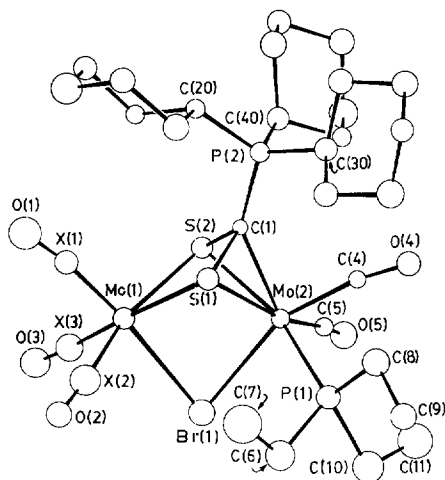


Fig. 1. Perspective view (CAMERON) [37] of the structure of one of the two independent molecules of **5a**, showing the atom numbering. The numbering of the atoms of the other molecule is related to that in the figure by adding 50.

1.33 g, 72%. Anal. Calcd. for $C_{21}H_{33}NO_3S_2PBrMo$: C, 40.83; H, 5.38; N, 2.26. Found: C, 41.22; H, 5.61; N, 2.22%.

3.2. Preparation of $[OC)_2(ON)Mo(\mu-Br)(\mu-S_2CPCy_3)M(CO)_3]$ (**4**)

A solution of freshly prepared $[Mo(CO)_3(NCMe)_3]$ (1.0 mmol) in THF (20 ml) was added to the suspension of complex **3** (0.62 g, 1.0 mmol) in THF (10 ml). After the reaction mixture was stirred at room temperature for 2 h, all brown suspension in the solution disappeared to give a clear, brown red solution. The solvent was pumped off over 3 h. The residue was extracted with CH_2Cl_2 /hexane (2:1, v/v) and filtered. The filtrate was concentrated slowly until about 5 ml. The supernatant was decanted and the brown red microcrystals (**4a**) were washed with hexane. Yield: 0.72 g, 90%. Anal. Calcd. for $C_{24}H_{33}NO_6S_2PBrMo_2$: C, 36.12; H, 4.17; N, 1.75. Found: C, 36.14; H, 4.22; N, 1.75%.

Complex **4b** was prepared, starting from **3** and $[W(CO)_3(NCMe)_3]$, by the same method described above. Yield of **4b**: 0.76 g, 86%. Anal. Calcd. for $C_{24}H_{33}NO_6S_2PBrMoW$: C, 32.54; H, 3.75; N, 1.58. Found: C, 32.69; H, 3.76; N, 1.59%.

3.3. Reactions of **4a** with PR_3

PEt_3 (30 μ l, 0.2 mmol) was added to a solution of **4a** (0.160 g, 0.2 mmol) in THF (15 ml). The mixture was stirred for 15 min, then the solvent was removed in vacuo. The deep red residue was redissolved in CH_2Cl_2 (10 ml) and the complex $[(OC)_2(ON)Mo(\mu-Br)(\mu-S_2PCy_3)Mo(CO)_2(PEt_3)]$ (**5a**) was isolated as red microcrystals by slowly evaporation of the solvent in vacuo. Yield: 0.17 g, 95%. The single crystals of **5a** for X-ray determination were obtained by recrystallization in CH_2Cl_2 /hexane (2:1, v/v). Anal. Calcd. for $C_{29}H_{48}NO_5S_2P_2BrMo_2$: C, 39.23; H, 5.45; N, 1.58. Found: C, 39.59; H, 5.58; N, 1.57%.

Complex **5b** was obtained as the method described above for **5a**, by using **4a** (0.2 g, 0.25 mmol) and $P(OMe)_3$ (31 μ l, 0.26 mmol). Yield: 0.21 g, 92%. Anal. Calcd. for $C_{26}H_{42}NO_8S_2P_2BrMo_2$: C, 34.94; H, 4.74; N, 1.57. Found: C, 35.15; H, 4.89; N, 1.65%.

3.4. Structure determination of **5a**

Crystals suitable for an X-ray determination were grown by slow diffusion of hexane into a concentrated solution of compound **5a** in CH_2Cl_2 . Relevant crystallographic details are given in Table 3. Unit cell parameters were determined from the least-squares refinement of a set of 25 centered reflections. Two standard reflections were monitored periodically, they showed no change during data collection. The structure was solved by direct methods with SHELX86 [34] and subsequent

Fourier maps. Two crystallographically independent, but chemically equivalent molecules were found in the asymmetric unit. Refinement and other computations were performed with CRYSTALS [35]. An absorption correction was applied with DIFABS [36]. Due to the low quality of the crystal, a low number of reflections were available for refinement. This was done in three blocks, keeping all atoms isotropic. Bond lengths and angles within the cyclohexyl groups had to be constrained to chemically reasonable values during the refinement, but in the last cycles these constraints were suppressed. The low accuracy of the structure made it impossible to distinguish between NO and CO groups. Therefore, the three atoms surrounding Mo(1) and Mo(51) were refined simultaneously as N (occupancy factor = 1/3) and C (occupancy factor = 2/3) in the same positions. The drawing of Fig. 1 was made with CAMERON [37].

3.5. Reactions of **4a** with diphosphines

A mixture of **4a** (0.2 g, 0.25 mmol) and dmpm (40 μ l, 0.25 mmol) in CH_2Cl_2 (6 ml) was stirred at room temperature for 20 min. Hexane (5 ml) was immediately added and the solution was slowly concentrated in vacuo until about 3 ml. The supernatant was decanted and the deep red microcrystals (**6a**) were washed with hexane. After dried in vacuo, the complex **6a** was stored in a refrigerator. Yield: 0.14 g, 62%. Anal. Calcd. for $C_{28}H_{47}NO_5S_2P_3BrMo_2$: C, 37.08; H, 5.23; N, 1.54. Found: C, 37.00; H, 5.95; N, 1.48%.

A mixture of **4a** (0.2 g, 0.25 mmol) and dppm (0.1 g, 0.25 mmol) in THF (20 ml) was stirred at room temperature for 8 h, and then the solvent was evaporated in vacuo. The red brown residue was redissolved in CH_2Cl_2 /hexane (1:1, v/v) and the solution was slowly concentrated in vacuo until about 5 ml. The deep red microcrystals (**6b**) were washed with diethyl ether and recrystallized in CH_2Cl_2 /hexane. Yield: 0.23 g, 80%. Anal. Calcd. for $C_{48}H_{55}NO_5S_2P_3BrMo_2$: C, 49.91; H, 4.80; N, 1.21. Found: C, 49.75; H, 4.86; N, 1.35%.

Acknowledgements

We are grateful to the Spanish Ministerio de Educación for financial support (Projects DGICYT PB91-0678 and PB94-1332) and for a grant to M.W. The authors wish also to thank Dr. Julio A. Pérez-Martínez for many helpful discussions.

References

- [1] H. Werner, W. Bertleff, Chem. Ber. 113 (1980) 267.
- [2] S.M. Boniface, G.R. Clark, J. Organomet. Chem. 188 (1980) 263.

- [3] P.K. Baker, K. Broadley, N.G. Connelly, *J. Chem. Soc. Dalton Trans.* (1982) 471.
- [4] T.R. Gaffney, J.A. Ibers, *Inorg. Chem.* 21 (1982) 2062.
- [5] W.A. Schenck, T. Schiwietzke, H. Muller, *J. Organomet. Chem.* 232 (1982) C41.
- [6] C. Bianchini, C. Ghilardi, A. Meli, S. Midollini, A. Orlandini, *Organometallics* 1 (1982) 778.
- [7] R. Usón, J. Forniés, R. Navarro, M.A. Usón, M.P. García, A.J. Welch, *J. Chem. Soc. Dalton Trans.* (1984) 345.
- [8] D. Miguel, V. Riera, J.A. Miguel, C. Bois, M. Philoche-Levisalles, Y. Jeannin, *J. Chem. Soc. Dalton Trans.* (1987) 2875.
- [9] D. Miguel, V. Riera, J.A. Miguel, F. Diego, C. Bois, Y. Jeannin, *J. Chem. Soc. Dalton Trans.* (1990) 2719, and references cited therein.
- [10] G. Barrado, J. Li, D. Miguel, J.A. Pérez-Martínez, C. Bois, Y. Jeannin, *Organometallics* 13 (1994) 2330, and references therein.
- [11] A. Galindo, E. Gutiérrez-Puebla, A. Monge, M.A. Muñoz, A. Pastor, C. Ruiz, E. Carmona, *J. Chem. Soc. Dalton Trans.* (1992) 2307.
- [12] C. Bianchini, A. Meli, *J. Chem. Soc. Dalton Trans.* (1983) 2419.
- [13] C. Bianchini, A. Meli, P. Dapporto, A. Tofanari, P. Zanello, *Inorg. Chem.* 26 (1987) 3677.
- [14] B. Alvarez, S. García-Granda, Y. Jeannin, D. Miguel, J.A. Miguel, V. Riera, *Organometallics* 10 (1991) 3005.
- [15] D. Miguel, J.A. Pérez-Martínez, V. Riera, S. García-Granda, *Organometallics* 13 (1994) 4667.
- [16] B. Alvarez, S. García-Granda, J. Li, D. Miguel, V. Riera, *Organometallics* 13 (1994) 16.
- [17] E. Carmona, E. Gutiérrez-Puebla, A. Monge, P.J. Pérez, L.J. Sánchez, *Inorg. Chem.* 28 (1989) 2120.
- [18] P. Legzdins, S.J. Rettig, L. Sánchez, *Organometallics* 4 (1985) 1470.
- [19] P. Legzdins, P.J. Lundmark, S.J. Rettig, *Organometallics* 15 (1996) 2988.
- [20] A.A.H. van der Zeijden, C. Sontag, H.W. Bosch, V. Shklover, H. Berke, D. Nanz, W. von Philipborn, *Helv. Chim. Acta* 74 (1991) 1194.
- [21] A.A.H. van der Zeijden, H.W. Bosch, H. Berke, *Organometallics* 11 (1992) 563.
- [22] D. Miguel, J.A. Pérez-Martínez, V. Riera, S. García-Granda, *Organometallics* 13 (1994) 1336.
- [23] A.P. Gaughan, B.L. Haymore, J.A. Ibers, W.H. Myers, T.E. Napper, D.W. Meek, *J. Am. Chem. Soc.* 95 (1973) 6859.
- [24] B.L. Haymore, J.A. Ibers, *Inorg. Chem.* 14 (1975) 3060.
- [25] A. Galindo, C. Mealli, J. Cuyás, D. Miguel, V. Riera, J.A. Pérez-Martínez, C. Bois, Y. Jeannin, *Organometallics* 15 (1996) 2375.
- [26] K. Nakamoto, *Infrared and Raman Spectra of Inorganic and Coordination Compounds*, 4th ed., John Wiley and Sons, New York, 1989, p. 309.
- [27] D. Miguel, J.A. Pérez-Martínez, V. Riera, S. García-Granda, *Organometallics* 12 (1994) 1394.
- [28] E.M. López, D. Miguel, J.A. Pérez-Martínez, V. Riera, *J. Organomet. Chem.* 467 (1994) 231.
- [29] D. Miguel, J.A. Pérez-Martínez, V. Riera, unpublished results.
- [30] D.A. Clark, D.L. Jones, R.J. Mawby, *J. Chem. Soc. Dalton Trans.* (1980) 565.
- [31] D. Miguel, J.A. Pérez-Martínez, V. Riera, S. García-Granda, *Angew. Chem. Int. Ed. Engl.* 31 (1992) 76.
- [32] D.P. Tate, W.R. Knipple, J.M. Augl, *Inorg. Chem.* 1 (1962) 433.
- [33] G.J. Kubas, L.S. van der Sluys, *Inorg. Synth.* 28 (1990) 30.
- [34] G.M. Sheldrick, SHELX86, Program for Crystal Structure Solution. University of Göttingen, Göttingen, 1986.
- [35] D.J. Watkin, J.R. Carruthers, P.W. Betteridge, CRYSTALS, An Advanced Crystallographic Computer Program, Chemical Crystallography Laboratory, Oxford University, Oxford, UK, 1989.
- [36] N. Walker, D. Stuart, *Acta Crystallogr.* A39 (1983) 158.
- [37] L.J. Pearce, D.J. Watkin, CAMERON; Crystallography Laboratory, Oxford University, Oxford, UK, 1992.